

Fault Detection Using Negative Selection and Genetic Algorithms

Anam ABID, Zia Ul HAQ, Muhammad Tahir KHAN

(*University of Engineering and Technology, Peshawar, Pakistan*)

Abstract: In this paper, negative selection and genetic algorithms are combined and an improved bi-objective optimization scheme is presented to achieve optimized negative selection algorithm detectors. The main aim of the optimal detector generation technique is maximal nonself space coverage with reduced number of diversified detectors. Conventionally, researchers opted clonal selection based optimization methods to achieve the maximal nonself coverage milestone; however, detectors cloning process results in generation of redundant similar detectors and inefficient detector distribution in nonself space. In approach proposed in the present paper, the maximal nonself space coverage is associated with bi-objective optimization criteria including minimization of the detector overlap and maximization of the diversity factor of the detectors. In the proposed methodology, a novel diversity factor-based approach is presented to obtain diversified detector distribution in the nonself space. The concept of diversified detector distribution is studied for detector coverage with 2-dimensional pentagram and spiral self-patterns. Furthermore, the feasibility of the developed fault detection methodology is tested the fault detection of induction motor inner race and outer race bearings.

Key words: Detector Coverage; Diversity Factor; Fault Detection; Genetic Algorithm; Negative Selection Algorithm

1 Introduction

Fault Detection (FD) has been an active research field for the last few decades. A variety of FD methods have been reported in the literature, ranging from model-based methods to intelligent computational methods. A detailed review of FD approaches can be found in [1-3]. Model-based techniques employ explicit mathematical models for the design of fault detection schemes such as in [4-7]. The potential of model-based fault detection methods is majorly associated with the availability of accurate mathematical models. For large, complex systems and in the presence of uncertain environment, the performance of model-based FD methods degrades. In order to cope with shortcomings of model-based methods, data driven or signal based fault detection approaches were also proposed by [8-10]. Data driven methods utilize large amounts of data related to the process history/trends and do not require a mathematical model.

In recent years, rapid increase has been seen in the development of biologically inspired techniques

such as artificial immune systems, evolutionary computation and genetic search, to solve engineering problems. The biological immune system is very complex and consists of many defense layers starting from the basic psychological instincts to composite networks of immune cells. The immune system has many interesting features and capabilities such as pattern recognition, learning, diversity maintenance, memory acquisition, distributed detection, and optimization^[11]. The capability of an immune system to distinguish the “self,” i.e., normal cells from the “nonself,” such as intruders and other pathogens is implemented primarily by two types of immune cells namely T-lymphocytes and B-lymphocytes. The T-lymphocytes are created in the bone marrow and further undergo a maturation process in thymus. During the maturation phase, T-lymphocytes pass through a negative selection process. Only those that do not match the self-proteins of the body are released out to circulate in the blood, while the self-reactive T-lymphocytes are destroyed.

Forrest^[12] presented the negative selection algorithm (NSA) based on the maturation mechanism of

T-lymphocytes. The development of real-valued NSA (RNSA) proved a paradigm shift in the research progress of NSA. RNSA was originally proposed by^[13] which employed real-valued vector for self-samples and detector representation. In recent years, many researchers have contributed to the development and improvement of NSA^[14-17]. NSA has been employed for many applications including anomaly detection^[17-18], robotics^[19], and aircraft fault detection^[20]. Research trend of combining NSA with other soft-computing techniques including sensor fusion^[21], genetic algorithms^[22-23], and particle swarm learning^[24-25] has been also reported in the literature. Gao^[22-23] introduced Genetic Algorithm (GA) and Clonal Selection Principle (CSP)-based optimized detector generation scheme with the aim to minimize the detector overlap. In their method, the clonal selection principle was utilized to enhance the number of detectors in the nonself space by creating clones of previously selected detectors. The major drawbacks of detector cloning are the lack of diversity and the presence of a large number of redundant detectors that result in ineffective nonself space coverage and poor detection performance.

Inspired by the incredible capabilities of genetic algorithm, the present paper investigates and elaborates on the features of GA for the improvement of NSA detector generation process. In contrast to^[23], implementation of this novel approach is independent of faulty behavior patterns that only require the healthy (fault-free) behavior of the system for the generation of GA optimized detectors. In the proposed approach, negative selection and genetic algorithms are combined and an improved bi-objective optimization method is incorporated to achieve optimized detectors. A novel diversity factor approach-based detector generation method is presented to obtain optimal, diversified detector distribution across the whole search space with reduced number of detectors. Furthermore, the nonself space coverage of the proposed scheme is examined with 2-dimensional (2D) pentagram and spiral patterns. In addition, the

fault detection performance of the proposed scheme is tested on inner race and outer race bearing faults of a motor. The healthy motor stator current signal is utilized for the generation of the GA optimized NSA detectors, and the resultant optimized detector set is used for fault detection.

The remaining paper is organized as follows: Section 2 describes the preliminary background of the negative selection algorithm and NSA detector optimization, and presents the problem formulation of bi-objective optimization-based NSA detector generation problem. In section 3, the proposed bi-objective genetic algorithm-based optimized detector generation method is presented, which particularly focuses on the diversity factor computation and the improved fitness function evaluation. Section 4 and 5 cover the computer simulation and the results where 2 dimensional (2D) self-pattern analysis and bearing fault detection examples are presented, respectively. Section 6 concludes the paper.

2 Preliminary Background

In this section, first an overview of the terminologies and the mathematical foundation of the primitive negative selection algorithm (NSA) is provided, followed by a brief discussion on the NSA detector generation process as an optimization problem. Furthermore, the limitations of the single objective optimization criterion selection in the detector generation process are explained, and finally the bi-objective optimization-based NSA detector generation problem is formally defined.

2.1 Overview of Negative Selection Algorithm (NSA)

The computational foundation of the negative selection algorithm is described now. A dataset representing the normal behavior of the system is gathered, known as the self-data. Afterwards, the candidate detectors are randomly generated and compared with the self-data. The detectors that do not match any sample of the self-data are retained and the remaining others are discarded.

Given “ M ” number of self-samples and “ N ” number of candidate detectors, let $O_i = [x_1^i, x_2^i \dots x_Q^i]$ and $o_j = [w_1^j, w_2^j \dots w_Q^j]$ represents a self-sample and a candidate detector, respectively, where $i = 1, 2 \dots M, j = 1, 2 \dots N$. Q is their common order and $x \in \mathbb{R}, w \in \mathbb{R}$ are real numbers. The matching degree between self-sample and candidate detector can be computed based on the Euclidean distance, according to

$$d = |O_i - o_j| = \sqrt{\sum_{q=1}^Q (x_q^i - w_q^j)^2} \quad (1)$$

Consequently, d is compared with a predefined threshold value λ (i.e., detector radius r_j). If $d > \lambda$, detector ‘ o_j ’ fails to match the self-sample ‘ O_i ’. A candidate detector becomes a valid detector and part of the Detector Set, if and only if, it does not match any self-sample. On the other hand, if $d < \lambda$, it is considered that the detector ‘ o_j ’ matches the self-sample ‘ O_i ’ and it is thus rejected. After a certain number of valid detectors are generated through the above mentioned procedure, these detectors are in turn used to detect anomaly in fresh samples.

2.2 Optimized NSA Detector Generation

Given an “ M ” number of self-samples, the goal of NSA is to generate detectors that cover the maximal nonself space with lesser number of detectors. In the NSA detector optimization problem, the decision variable is the center location of the detector $o^j = [w_1^j, w_2^j \dots w_Q^j]$ where $j = 1, 2 \dots N$. The detector location is optimized to ensure efficient non-self space coverage, employing minimum overlap between detectors as the optimization criterion. To elaborate, suppose that for a candidate detector centered at o_j with arbitrary radius r^j , O_k be the location of the nearest self-sample with self-radius R_k , as shown in Fig. 1. The detector’s distance from its nearest self-sample can be defined as,

$$|O_k - o_j| = \min_i^N |O_i - o_j| \quad (2)$$

and its maximal radius can be defined as,

$$r^j = |O_k - o_j| - R^k \quad (3)$$

where

$$|O_k - o_j| = \sqrt{\sum_{q=1}^Q (x_q^k - w_q^j)^2}$$

and

$$|O_i - o_j| = \sqrt{\sum_{q=1}^Q (x_q^i - w_q^j)^2}$$

The nearest-self distance depends upon the detector’s center o_j , which has vital importance in the formulation of the objective function. For any detector o_j with detector radius r^j , if there is self-sample O_i of self-radius R^i , such that $|O_i - o_j| \leq R^i$, then detector o_j overlaps with self-sample O_i and thus becomes an invalid detector. Therefore, the maximum radius of a valid detector is restricted by the location of its nearest-self sample, as illustrated in Fig. 1. Generally, it is suggested that the detector radius should be selected as ^[22],

$$r_j = \max_{o_j} |O_k - o_j| - R^k \quad (4)$$

Equation (4) describes the possible maximal detector radius for a valid detector centered at location o_j . In order to provide maximum nonself coverage with few numbers of detectors, the detector radius should be as large as possible. As the objective is to maximize the detector radius, equation (4) defines the basic objective function and it depends on the radius of nearest self-sample (generally fixed) and the nearest self-distance.

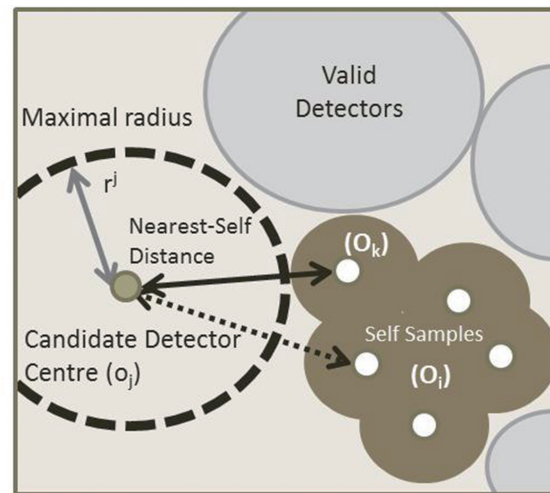


Fig. 1 Relationship between nearest-self distance and detector radius.

For each detector to be valid, it must satisfy the constraints:

$$|O_i - o_j| \geq R^i \quad \forall i, \forall j \quad (5)$$

Also each Q -dimensional detector must satisfy the real-valued boundary constraints as described by,

$$\begin{aligned} w_1^{lower} \leq w_1^j \leq w_1^{upper} \\ w_2^{lower} \leq w_2^j \leq w_2^{upper} \\ \vdots \\ w_Q^{lower} \leq w_Q^j \leq w_Q^{upper} \quad \forall j \end{aligned} \quad (6)$$

2.3 Bi-objective Optimization Problem Formulation

Previously, clonal selection and single objective-based optimization methods were presented to achieve the maximal nonself space coverage; however, detector cloning process results in the generation of redundant similar detectors and inefficient detector distribution in the nonself space. The aim of optimal NSA detector generation techniques is maximal nonself space coverage with reduced number of detectors, and at the same time covering the maximum types of anomalies. To address the aforementioned objectives and shortcomings of existing methods, there is a need to develop an effective detector generation and distribution strategy. In contrast to single optimization criterion or incorporation of multi-level optimization techniques, a bi-objective optimization method is suggested, focusing on minimizing the detector overlap and enhancing the detector diversity. The problem definition of bi-objective optimization-based NSA detector generation may be formally stated as follows:

Optimization goal:

“Maximal nonself space coverage”

Step:

“Determine the optimal detectors”

o_j (center location) and r_j (influence region)

Bi-objective criteria:

Minimization of detectors' overlap

Maximization of detectors' diversity

factor

The goal is to obtain diversified detectors across the whole search space with least number of optimally distributed detectors. The in-built diversification capabilities will limit the concentration of the generated detectors within a limited nonself region.

3 Proposed Method

In the present work, a bi-objective GA optimization-based NSA detector generation method is developed. To ensure efficient distribution of the detectors in the nonself space, the detector set should cover maximum number of anomalies (diversified nonself space coverage) and the detector overlap should be minimized. Hence, the present optimization goal is twofold: determination of the optimal o_j and r^j to achieve 1) diversified nonself space coverage, and 2) minimal detectors' overlap, simultaneously. In addition, the developed fault detection scheme is independent of fault patterns and requires only the knowledge of the normal behavior of the system to generate optimized NSA detectors. For the detector set generation, in contrast to classical generation-elimination strategy, GA optimized detector generation method is incorporated, as shown in Fig. 2. Its details are discussed next.

3.1 Bi-objective Optimization Criteria

The detector generation method focuses on nonself coverage with minimum number of detectors that are highly diversified to cover maximum types of anomalies. The detector generation mechanism is based on determination of the optimal detector center to maximize the detector influence region (radius) and the diversity aspect, with the constraint of self-matching detector prohibition. The proposed diversity factor-based fitness value evaluation enforces detector diversification across the whole search space. Fig. 3 illustrates the proposed bi-objective fitness value evaluation scheme based on the following criteria:

1. Detector overlap minimization

2. Diversity factor maximization

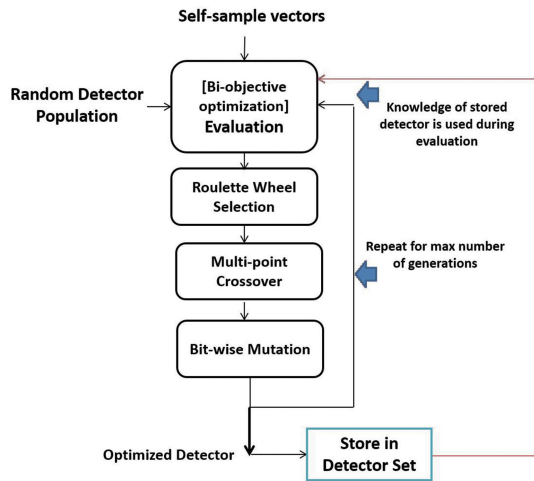


Fig. 2 GA optimized negative selection algorithm.

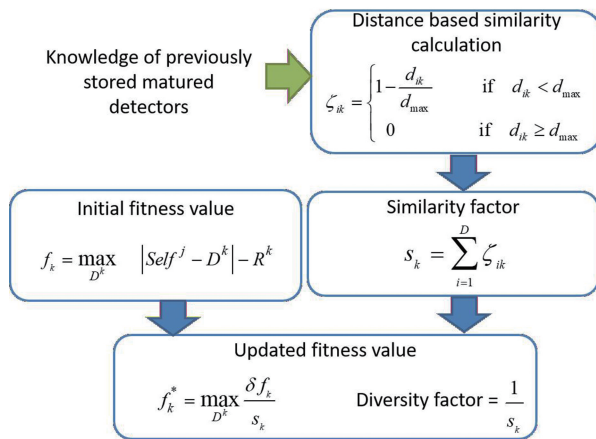


Fig. 3 Bi-objective fitness value evaluation scheme.

The objective (i) is achieved by the maximization of (4), which gives the initial fitness value of the candidate detector ' f_j ', and objective (ii) is achieved by the maximization of (7), which gives the updated fitness value ' f_j^* ', as

$$\max_{o_j} f_j^* = \max_{o_j} \frac{\delta f_j}{s_j} = \max_{o_j} \frac{\delta(|O_k - o_j| - R^k)}{s_i} \quad (7)$$

$$s_i = \sum_{j=1}^D \zeta_{ij} \quad (8)$$

where f_j , f_j^* and s_j are the initial fitness value, updated fitness value and similarity factor value, respectively. The δ is the scaling factor, which controls the influence of the diversity factor on the updated fitness value. The proposed method involves 3 steps: First, the knowledge of the previously stored optimized detector set is used for calculation of the

diversity factor ($1/s_j$) of the candidate detector, which utilizes the distance-based metrics ζ_{ij} for similarity assessment of the candidate detectors. Afterwards, initial fitness value based on r^j maximization is obtained using (4). Finally, the initial fitness value and the similarity factor are used to calculate the final updated fitness value of the candidate detector using (7). The detailed discussion on diversity factor computation for an arbitrary detector generation scenario is presented next.

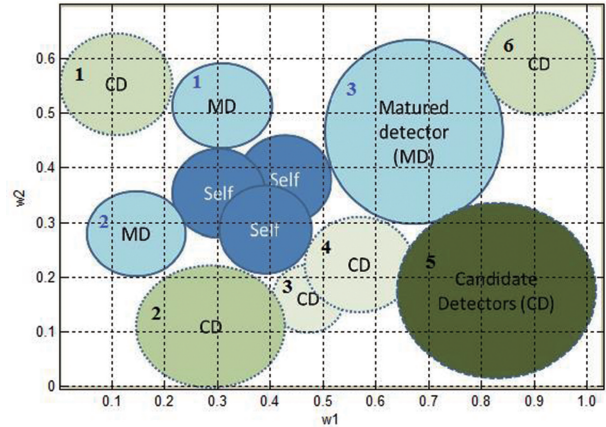


Fig. 4 Arbitrary detector distribution in 2D nonself space.

Table 1 Similarity values of candidate detectors.

ζ_{ij}	j = 1	j = 2	j = 3
i = 1	0.8600	0.8084	0.5970
i = 2	0.7091	0.8411	0.6248
i = 3	0.7218	0.7555	0.7349
i = 4	0.7210	0.6964	0.8090
i = 5	0.5601	0.5106	0.7666
i = 6	0.5693	0.4132	0.8134

3.2 Diversity Factor Computation

Consider a 2-dimensional (2D) region of space, with self and nonself space segments, as shown in the Fig. 4. Suppose that, D number of detectors have already been generated and selected through GA-based detector generation technique, denoted by MD (matured detectors). The self and nonself space distribution along with the location and influence region (radius) of matured detectors is il-

illustrated in Fig. 4. In order to generate another mature detector, a population of candidate detectors (CD) is generated. Fig. 4 shows a candidate detector population (size, $S = 6$) with their potential influence region. The potential influence region depends on the radius of the detector that is computed using equation (2) and (3). In the proposed bi-objective fitness evaluation method, to ensure the employment of diversity aspect-controlled generation of detectors, each candidate detector is assigned a similarity and diversity factor value that is based on the distance-based similarity metric of the candidate detector and the previously stored matured detectors.

The similarity values of all 6 candidate detectors in regard to 3 matured detectors are given in Table 1. The similarity value depends on the phenotypic dis-

Table 2 Comparison of initial fitness value, similarity factor and updated fitness value of candidate detectors.

Candidate Detector #	Initial fitness value (f_i)	Similarity factor (s_i)	Updated fitness value (f^{share})
$i = 1$	0.189	2.2654	0.117
$i = 2$	0.225	2.1751	0.146
$i = 3$	0.123	2.2122	0.078
$i = 4$	0.177	2.2264	0.112
$i = 5$	0.322	1.8373	0.247
$i = 6$	0.191	1.7959	0.150

The evaluation process of candidate detectors is based on the updated fitness value that considers both the largest radius and the most diversified nature of the detectors. The proposed method assigns lower fitness values to the candidate detectors # 3 and #4 and the highest fitness value to the candidate detector # 5. The resultant updated fitness values in Table 2 support the intuitive candidate detector ranking based on bi-objective evaluation criteria. The method intends to obtain an appropriate collection of diverse detectors that attempt to locate themselves far apart from matured detectors (i.e., already selected).

In essence, with the incorporation of similarity factor, the amount of reduction in fitness value of the candidate detector is proportional to the sum of its phenotypic resemblance with other matured detec-

tance between the individual candidate detector and the matured detector. The relationship between the phenotypic distance and the similarity value is mathematically defined as,

$$\zeta_{ij} = \begin{cases} 1 - \frac{d_{ij}}{d_{max}} & \text{if } d_{ij} < d_{max} \\ 0 & \text{if } d_{ij} \geq d_{max} \end{cases} \quad (9)$$

(not a valid detector)

where d_{max} is the distance between the upper and lower limits. The similarity factor value for an individual i is defined as the sum of the individual similarity values (ζ_{ij}) between i th candidate detector and all other ‘ D ’ number of matured detectors, as given in (8). Table 2 lists the similarity factor values, initial fitness value and the updated fitness values of all the candidate detectors.

In other words, the higher fitness value of candidate detector represents its high diversity aspect. The role of the diversity factor is to reduce the fitness of those candidate detectors who have a large number of close relations (phenotypic) within the detector population. This limits their chance to become part of the next generation and ultimately their selection as the new matured detector. In summary, the proposed bi-objective optimization method encourages the exploration of diversified detectors and generates an optimally distributed detector set.

3.3 GA Implementation

The architecture of proposed GA-based optimized detector generation method is shown in Fig. 1. It utilizes the bi-objective evaluation function described in (7). This section describes the employed

GA operators and stepwise implementation details of the algorithm.

First, a penalty function is incorporated with the aim to reduce the fitness value of an individual in case the individual violates one or more constraints (5) and (6). The amount of reduction in the fitness value is generally proportional to the number of violations. The proposed genetic algorithm configuration employs simple roulette wheel or fitness proportionate selection scheme. With this approach, the probability of selection is proportional to an individual's fitness. A parameter P_c is defined, which decides the probability of the bit exchange. For the multi-parameter problem (multiple unknowns), generally the crossover cut point (c_{point}) does not lie between parameters but within a parameter. However, in the problem under consideration, the binary sub-strings are concatenated to form a chromosome of length L , and the crossover points can be at any locus numbers between 1 and $L-1$. To implement the bitwise mutation with each new generation, the whole population is swept with every bit position in every string visited and very occasionally (with a small probability P_M) a '1' is flipped to a '0' and vice versa. The probability of mutation P_M is usually very small. With the implementation of elitism operator, the progression of elite member within the population is ensured. The elite member is not only selected but also ensures that its copy is not disrupted by crossover or mutation.

The termination criteria opted in the proposed GA architecture is the maximum number of generations. After a pre-specified number of generations, an optimized matured detector is generated. The center location and the radius of the optimized detector are stored in the matured detector set. Furthermore, the matured detector set is included in the self-sample set, and the updated self-sample set is used for generation of the next matured detector. The process is repeated until the required numbers of matured detectors are generated. The inclusion of matured detectors and the incorporation of updated self-sample

set ensure minimum overlapping between the previously stored matured detectors and the future detector candidates.

4 Simulation and Results

In order to evaluate the performance of the proposed genetic algorithm-based NSA detectors, simulations are performed. The simulations involved two types of examples including 2D pentagram and spiral self-patterns. The simulation and results are discussed in this section.

4.1 2D Self-patterns and Simulation Parameters

To observe the detector coverage, it is considered appropriate to test the developed algorithm with 2 dimensional (2D) patterns. In 2D pattern analysis, the self-space is represented by data points with regular-shaped pentagram and spiral, as illustrated with dark circles in Fig. 5 and Fig. 6, respectively. For the generated self-space, GA optimized NSA detectors are generated using the developed scheme. For the 2D pattern detector coverage of both pentagram and spiral-based self-patterns, the order of the detectors is defined as $Q = 2$. Table 3 lists the parameters used in the simulation.

Table 3 List of Parameters for 2D pattern analysis.

Simulation Parameter	Symbol	Pentagram	Spiral
Substring length	l_1	5	8
Substring length	l_2	5	8
Mutation probability	P_M	0.1	0.2
Crossover probability	P_C	0.8	0.8
No. of crossover points	c_{point}	3	4
r_{min} of $q = 1$	w_{1Lower}	-2	-3
r_{min} of $q = 2$	w_{2Lower}	-2	-7
r_{max} of $q = 1$	w_{1Upper}	1.5	6
r_{max} of $q = 2$	w_{2Upper}	1.5	3
Population size	S	20	20

4.2 Detector Coverage

For the pentagram case, the self-space consists of $M = 450$ self-samples with self-radius of $r^{self} = 0.05$. With the implementation of the developed approach, $N = 15$ GA optimized detectors are genera-

ted. As it is evident from Fig. 5, that GA optimized detectors show good diversified coverage and provides almost 90% of nonself space coverage.

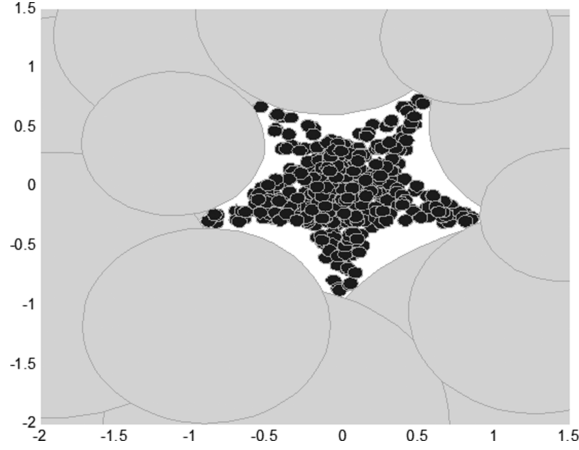


Fig. 5 Detector coverage with pentagram self-pattern.

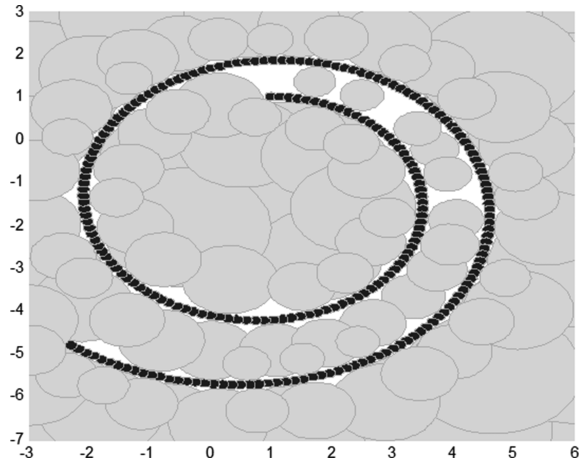


Fig. 6 Detector coverage with spiral self-pattern.

For spiral self-space pattern, a total of $M = 220$ self-samples with self-radius of $r^{self} = 0.1$ are generated. With the implementation of the developed approach, $N = 100$ optimized detectors are generated. Depending on the complex nature of the self-space, an increase in the number of detectors could be observed. In addition, GA optimized detector set consists of few small-sized detectors, as illustrated in Fig. 6. It is worthy to note that the proposed approach is intelligent enough to consider the nature of the self-space and provide optimal coverage with diversified detector set.

5 Bearing Fault Detection

Induction motors are commonly used in a wide range of applications and are often subjected to different types of faults. Bearing faults contribute a major share (40%) of the total faults of the motors^[26]. Bearing faults occur due to inner race, outer race or ball defects. In order to investigate the fault detection performance of the proposed optimized NSA detector generation scheme, it is tested under inner race and outer race bearing faults.

In fault-free induction motors, the stator current consists of the 1st and 3rd harmonics whose amplitude depends on the motor rating and the load. Hussein^[27] investigated that the effect of bearing fault can be modeled as an additional bearing current component in the normal (healthy motor) stator current. This faulty current component contains frequency harmonics. In case of outer and inner race bearing faults, the stator current contains this additional current due to the harmonics calculated by the following equations:

$$f_v = \left(\frac{N_b}{2}\right) f_r \left[1 - b_d \frac{\cos(\beta)}{b_p} \right] \quad (14)$$

$$f_v = \left(\frac{N_b}{2}\right) f_r \left[1 + b_d \frac{\cos(\beta)}{b_p} \right] \quad (15)$$

where N_b is the total number of balls, b_d is the ball diameter, b_p is the ball pitch diameter, and β is the contact angle of the ball with the races. A detailed description can be found in^[27, 28].

5.1 Collection of Self-samples

The proposed fault detection approach is independent of the fault types and patterns, and for the optimized NSA detector generation only the healthy behavior of the system (i.e., motor stator current) is required. In the present study, ACS712ELCTR current sensor module is employed for the measurement of the stator current, which has a 5A input current range and a 185mV/A sensitivity. The current sensor produces a proportional signal with an accuracy of 1.5% and 5V maximum output. The feature signal time series of the current signal of a healthy

motor is shown in the upper portion of Fig. 7 (a).

Initially, a total of 2000 sampled data points of the healthy motor stator current are collected. Subsequently, these sampled points are segmented into non-overlapping frames of width Q . With the same healthy motor current sampled points and with different window-widths, two sets of frames were produced; i.e., by setting $Q = 8$ and 10. By setting $Q = 8$, a total of $2000/8 = 250$ frames were produced. By setting $Q = 10$, a total of $2000/10 = 200$ frames were produced. These two sets of self-samples (Self-sample Set 1 and Self-sample Set 2) were utilized in the two sets of experiments as presented next.

5.2 GA Optimized Detector Set Generation

After the collection of the self-sample sets, optimized NSA detectors are generated. In this example, for each self-sample set (Self-sample Set 1 and Self-sample Set 2) respective detector set (Detector Set 1 and Detector Set 2) is generated. Each pair of self-sample and detector set consists of real-valued vectors of pre-defined vector size. For Self-Detector Pair 1: vector size of each self-sample is $Q = 8$ and self-radius $r^{self} = 0.01$, and detectors of the same size, i.e., $Q = 8$ are generated. Similarly, for Self-Detector Pair 2: vector size of each self-sample is $Q = 10$ and self-radius $r^{self} = 0.03$, and detectors of the same size, i.e., $Q = 10$ are generated. For the implementation of the algorithm, the list of parameters used for the generation of two detector sets is given in Table 4.

5.3 Testing and Fault Detection Results

In the validation phase, a total of 2000 fresh sampled data points are collected. This new validation sampled data consists of faulty current (inner/outer bearing fault) sampled values and normal (fault-free) current sampled values. Subsequently, these sampled points are segmented into non-overlapping frames of width Q . With the same validation data sampled points and with different window-widths, two sets of frames were produced; i.e., by

setting $Q = 8$ and 10.

By setting $Q = 8$, a total of $2000/8 = 250$ test frames are produced, each representing a real-valued test-sample vector. The beginning 125 test-samples are faulty (1000th sample number) and the remaining 125 samples represent the normal behavior of the motor, as shown in Figure 7. By setting $Q = 10$, a total of $2000/10 = 200$ frames are produced. The beginning 100 test-samples (1000th sample number) represent faulty behavior and the remaining 100 test-samples are normal (healthy) samples, as shown in Fig. 7 and Fig. 8 for the inner race and the outer race bearing faults, respectively. These two validation sets of test-samples are utilized to examine the fault detection performance of Detector Set 1 and Detector Set 2, respectively.

For fault detection in the induction motor, test samples are matched with GA optimized detectors. The test-sample and detector matching is based on a distance metric and is mathematically described as follows:

Let d be the distance between the i^{th} -Test sample (T_i) and the j^{th} -Detector (o_j, r_j),

$$T_j = [t_1^j, t_2^j \cdots t_Q^j] \quad , o_j = [w_1^j, w_2^j \cdots w_Q^j]$$

$$d_{ij} = |T_i - o_j| = \sqrt{\sum_{q=1}^Q (t_q^i - w_q^j)^2} \quad (16)$$

If $d_{ij} > r^j$ for any j^{th} -detector ($j = 1, 2, \dots, N$), it indicates that the i^{th} -Test sample is faulty.

With the aforementioned detector-test sample matching criteria, the bearing fault detection is performed on the test samples. The fault detection results are shown in Fig. 7 (a, b) and Fig. 8 (a, b) for the inner race ($Q = 8, 10$) and the outer race ($Q = 8, 10$) bearing faults, respectively. For performance assessment of the developed method fault detection rate (FDR) and false alarm rate (FAR) are used. Let A and B denote the total misdetected healthy frame and the total detected faulty frames, respectively.

$$\text{FDR} = B / \text{Total faulty frames}$$

$$\text{FAR} = A / \text{Total healthy frames}$$

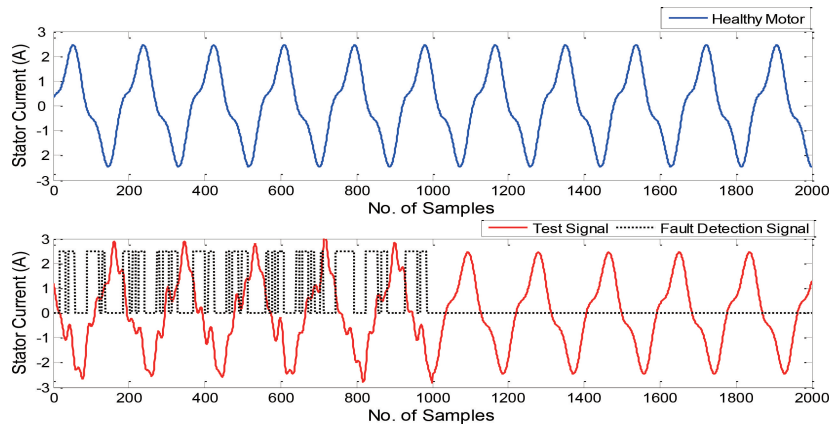


Fig. 7(a) Inner Race Bearing fault detection with order $Q = 8$.

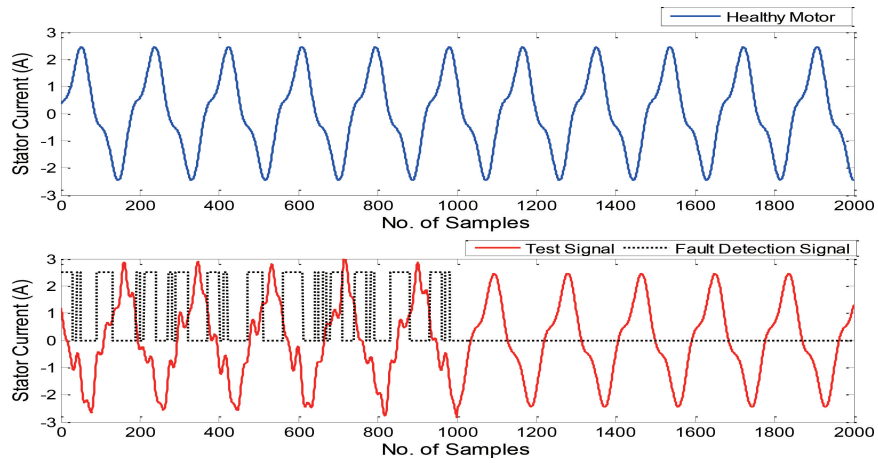


Fig. 7(b) Inner Race Bearing fault detection with order $Q = 10$.

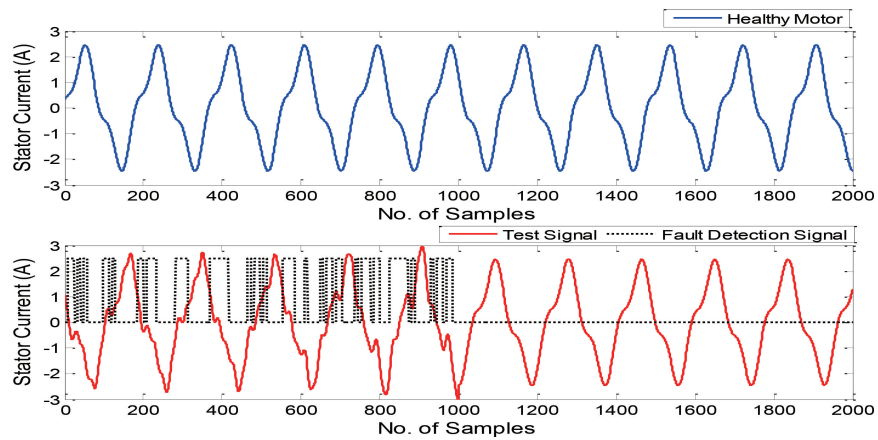


Fig. 8(a) Outer Race Bearing fault detection with order $Q = 8$.

The FDR and FAR for the inner and outer race bearing faults and with variation in the frame window-width (order Q) are listed in Table 5. For each

combination, simulations are carried out and the effect of the window-width variation on FDR and FAR is studied. The developed fault detection

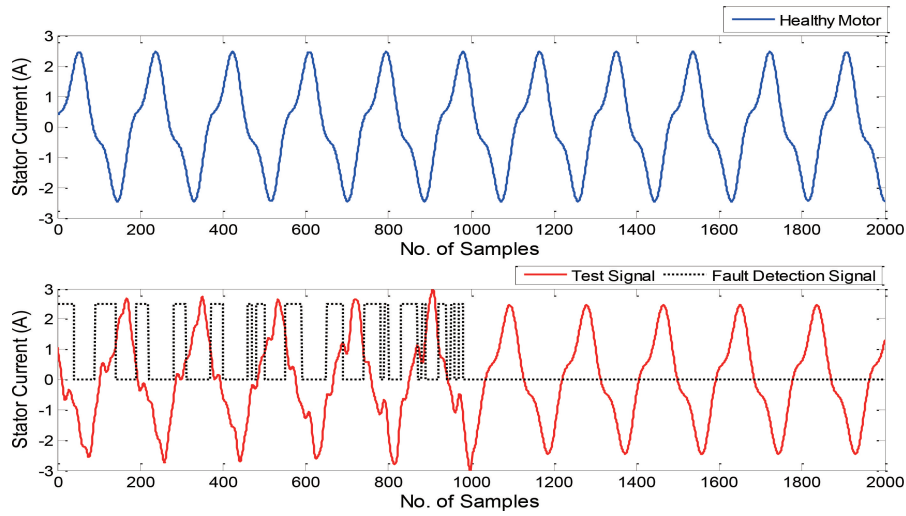


Fig. 8(b) Outer Race Bearing fault detection with order $Q = 10$.

scheme has the ability to effectively indicate the faulty behavior (bearing fault) with good fault detection rate, i.e., 81.6 % (inner race fault) and 75.2% (outer race fault) and excellent FAR of 0% in all the cases. In the bearing fault detection example, the appropriate segment boundary or window-width is chosen on the basis of improved fault detection accuracy using trial and error method. In the present study, the best fault detection performance is achieved with $Q = 10$. In addition, the determination of the appropriate window-width also depends on the signal dynamics or the distribution of the frequency contents within the signal. For periodic signals with generally slow dynamic variations, constant or uniform windowing methods are recommended.

However, depending on the system behavior,

an appropriate window-width should be selected. A very small window-width may not be able to capture the significant patterns to distinguish normal and faulty system behavior. Similarly, a very large window-width may result in false alarm and lead to increase in the computational complexity.

Table 4 List of Parameters for bearing fault detection.

Parameter	Symbol	Value
Substring length	$l_q (q = 1, 2, \dots, Q)$	6
Lower bound (ymin)	$w_q^{Lower} (q = 1, 2, \dots, Q)$	-3
Upper bound (ymax)	$w_q^{Upper} (q = 1, 2, \dots, Q)$	3
Population size	S	30
Mutation probability	P_M	0.2
Crossover probability	P_C	0.8
No. of crossover points	c_{point}	4

Table 5 Bearing Fault Detection Analysis.

Fault	Order	No. of GA	Total	Total	Fault	False Alarm Rate
		Optimized NSA Detectors	Misdetected Healthy Frames	Detected Faulty Frames	Detection Rate	
	Q	N	A	B	FDR	FAR
Inner race	8	60	0	102	81.6%	0%
	10	60	0	74	74%	0%
Outer race	8	60	0	94	75.2%	0%
	10	60	0	66	66%	0%

6 Conclusion

In this paper, a novel fault detection scheme was presented combining genetic and negative selection algorithms. In the proposed approach, the maximal nonself space coverage was achieved through bi-objective optimization criteria including minimization of the detector overlap and maximization of the detector diversity factor. The main aim of bi-objective optimal detector generation technique was maximal nonself space coverage with reduced number of diversified detectors. In the proposed methodology, a diversity factor was utilized to obtain a diversified detector distribution in the nonself space. The developed scheme was tested with inner and outer race bearing fault detection, and the detector nonself space coverage was studied with 2D self-pattern analysis. The simulation results supported the claimed fault detection capabilities of the developed method.

References

- [1] Venkatasubramanian, V. (2003). A review of process fault detection and diagnosis Part I, II, III. *Comput. Chem. Eng.* 27, pp. 293-346.
- [2] Henriquez, P. (2014). Review of Automatic Fault Diagnosis System Using Audio and Vibration Signals. *IEEE Trans. Syst. Man Cybern. Syst.* 44(5), pp. 642-652.
- [3] Hekmat, S. (2016). Real Time Fault Detection and Isolation: A comparative study. *Int. J. Comput. Appl.* 134(6), pp. 8-15.
- [4] Gajanayake, C. (2013). Sensor fault detection, isolation and system reconfiguration based on extended Kalman filter for induction motor drives, *IET Electr. Power Appl.* 7(7), pp. 607-617.
- [5] Kawashima, H. (2003). A Multi-Model Based Fault Detection and Diagnosis of Internal Sensor for Mobile Robot. *Conf. on Intelligent Robots and Systems Las Vegas*. pp. 3787-3792.
- [6] Arogeti, SA. (2009). Fault Detection and Isolation in a Mobile Robot Test-bed. *IEEE/ASME Int. Conf. on Advanced Intelligent Mechatronics, Suntec Convention and Exhibition Center Singapore*. pp. 398-404.
- [7] Tabbache, B. (2013). Virtual-Sensor-Based Maximum-Likelihood Voting Approach for Fault-Tolerant Control of Electric Vehicle Powertrains. *IEEE Trans. Veh. Technol.* 62(3), pp. 1075-1083.
- [8] Yu, C. (2008). A Kernel-Based Bayesian Classifier for Fault Detection and Classification. *World Congr. on Intelligent Control and Automation*. 1, pp. 124-128.
- [9] Chen, YM. (2002). Neural networks-based scheme for system failure detection and diagnosis. *Math. Comput. Simul.* 58, pp. 101-109.
- [10] Jain, AA. (2000). A neural network based actuator fault detection and diagnostic scheme for a SCARA manipulator. *IEEE Int. Symposium on Intelligent Control*. pp. 297-302.
- [11] Castro, LND. (1999). Artificial Immune Systems; Part I- Basic Theory and Applications. *Universidade Estadual de Campinas, Dezembro de, Tech. Rep* 210, pp. 1-15.
- [12] Forrest, S. (1994). Self-Nonself Discrimination in a Computer. *IEEE Symposium on Research in Security and Privacy, Los Alamitos, CA*. pp. 202-212.
- [13] Gonzalez, L. (2003). A randomized real-valued negative selection algorithm. *Proceedings of the 2nd International Conference on Artificial Immune Systems (ICARIS)*. LNCS, Edinburgh, UK, Springer-Verlag. pp. 261-272.
- [14] Gonz, FA. (2004). Anomaly Detection Using Real-Valued Negative, Genet. Program. *Evolvable Mach.* 4(4), pp. 383-403.
- [15] Laurentys, CA. (2010). Design of an Artificial Immune System for fault detection; A Negative Selection Approach. *Expert Syst. Appl.* 37(7), pp. 5507-5513.
- [16] Silva, GC. (2012). Immune inspired Fault Detection and Diagnosis; A fuzzy-based approach of the negative selection algorithm and participatory clustering. *Expert Syst. Appl.* 39(16), pp. 12474-12486.
- [17] Abid, A. (2018). Layered and Real-valued Negative Selection Algorithm for Fault Detection. *IEEE Syst. J.* 12(3), pp. 2960-2969.
- [18] Gao, XZ. (2013). A study of negative selection algorithm-based motor fault detection and diagnosis. *Int. J. Innov. Comput. Inf. Control.* 9(2), pp. 875-901.
- [19] Canham, R. (2003). Robot Error Detection Using an

- Artificial Immune System. *NASA/Dod Conf. on Evolvable Hardware*. pp. 199-207.
- [20] Dasgupta, D. (2004). Negative Selection Algorithm for Aircraft Fault Detection. *Artif. Immune Syst. Springer Berlin Heidelb.* pp. 1-3.
- [21] Abdel, M. (2009). A Hybrid Intelligent System for Fault Detection and Sensor Fusion. *Appl. Soft Comput.* 9, pp. 415-422.
- [22] Abid, A. (2020). Multidomain Features-based GA Optimized Artificial Immune System for Bearing Fault Detection. *IEEE Trans. Syst. Man Cybern. Syst.*, 50 (1), pp. 348-359.
- [23] Gao, XZ. (2010). Multi-Level Optimization of Negative Selection Algorithm Detectors with Application In Motor Fault Detection. *Intell. Autom. Soft Comput.* 16(3), pp. 353-375.
- [24] Ye, L. (2013). An Artificial Immune Classification Algorithm based on Particle Swarm Optimization. *J. Comput.* 8(3), pp. 772-778.
- [25] Aydin, I. (2010). Artificial Immune classifier with Swarm Learning, *Eng. Appl. Artif. Intell.* 23, pp. 1291-1302.
- [26] Schoen, RR. (1995). Motor bearing damage detection using stator current monitoring. *IEEE Trans. Ind. Appl.* 31, pp. 1274-1279.
- [27] Hussein, NA. (2012). 3-phase Induction Motor Bearing Fault Detection and Isolation using MCSA Technique based on neural network Algorithm. *J. Eng. Dev.* 16(3), pp. 175-189.
- [28] Blödt, M. (2008). Models for Bearing Damage Detection in Induction Motors Using Stator Current Monitoring. *IEEE Trans. Ind. Electron.* 55 (4), pp. 1813-1822.

Authors' Biographies



Anam ABID received her Bachelor's degree in electrical engineering from the University of Engineering and Technology, Peshawar, Pakistan, and the Master's degree in electrical engineering from the National University of Sciences and Technology, Pakistan. She is currently pursuing her Ph.D. degree in Mechatronics and holds a faculty position with the Department of Mechatronics Engineering at the University of Engineering and

Technology, Peshawar. Her research interests include fault detection, control systems, machine learning, and signal processing.



Zia Ul HAQ received his Bachelor's degree in agricultural engineering and Master's degree in soil and water engineering from NWFP University of Engineering and Technology, Peshawar, Pakistan, and Ph.D. degree from the University of Southampton, UK, in 1996, 2003, and 2009, respectively. Currently, he is an Assistant Professor with the Department of Agriculture at the University of Engineering and Technology, Peshawar, Pakistan. His research interests include soil and water engineering, irrigation, and intelligent computing methods.



Muhammad Tahir KHAN received his Bachelor's degree in mechanical engineering from NWFP University of Engineering & Technology, Peshawar, Pakistan, Master's degree in mechatronics from University of New South Wales, Sydney, Australia, and Ph.D. degree from the University of British Columbia, Vancouver, BC, Canada, in 1997, 1999, and 2010, respectively. He was a postdoctoral fellow with the Industrial Automation Laboratory at the University of British Columbia, Vancouver, BC, Canada for 2 years until January 2012. Currently, he is a Professor with the Department of Mechatronics at the University of Engineering and Technology, Peshawar, Pakistan. His research interests include robotics, and intelligent control systems.

